JOURNAL OF RHEOLOGY

Apparent elongational yield stress of soft matter

L. Martinie, H. Buggisch, and N. Willenbacher

Citation: J. Rheol. **57**, 627 (2013); doi: 10.1122/1.4789785

View online: http://dx.doi.org/10.1122/1.4789785

View Table of Contents: http://www.journalofrheology.org/resource/1/JORHD2/v57/i2

Published by the The Society of Rheology

Apparent elongational yield stress of soft matter

L. Martinie, H. Buggisch, and N. Willenbacher[a)]

Institute of Mechanical Process Engineering and Mechanics, Karlsruhe Institute of Technology, Karlsruhe 76131, Germany

(Received 15 May 2012; final revision received 28 December 2012; published 4 February 2013)

Synopsis

Apparent elongational yield stresses of soft matter including polymer gels, highly concentrated emulsions, and aggregated suspensions have been determined from step stretch experiments. Materials display apparent shear yield stresses in the range 1–100 Pa and large but finite shear relaxation times t_R. For all investigated fluids, the Laplace pressure within the stretched filaments is essentially constant during an initial period of time after the step strain. Then, it increases rapidly and finally the filaments break. Filament lifetime t_f strongly increases with decreasing stretching ratio ε. The apparent elongational yield stress is identified as the initial value of the Laplace pressure obtained at a critical stretching ratio ε_c corresponding to a Deborah number $De = t_R/t_f = 1$. For all fluids, the ratio of this elongational yield stress to shear yield stress is $\sqrt{3}$ in agreement with the von Mises plasticity criterion, irrespective of the physical nature of structural breakdown. Elongational experiments performed at different ε or t_f covering Deborah numbers between 0.1 and 100 reveal a universal relationship between the initial plateau value of the Laplace pressure normalized to the shear yield stress and De. This stress ratio varies between 0.5 and 5, and equals $\sqrt{3}$ only for $De \approx 1$. © *2013 The Society of Rheology*. [http://dx.doi.org/10.1122/1.4789785]

I. INTRODUCTION

A broad variety of soft matter including dispersions, emulsions, and foams, with attractive particle/droplet interactions and/or dense particle/droplet packing exhibit a so-called apparent yield stress. The physical nature and proper characterization of the apparent yield stress is still a matter of debate due to the large variety of materials concerned. For certain fluids, the yield stress represents a transition from a solid to a liquid state and, similar to the behavior of solids, the deformation at stresses below τ_y is purely elastic [Hartnett and Hu (1989)]. For other materials, the apparent yield stress is a transition between two liquid phases with very different viscosities [Barnes (1999)] and even if the shear viscosity at $\tau < \tau_y$ is independent of the applied stress, it can be time variant [Moller *et al.* (2009)]. Moreover, yield stress fluids may exhibit a "thixotropic" response due to the dynamic adjustment of the microstructure to the applied macroscopic stress, and shear banding or other flow discontinuities are observed even below τ_y [Bonn and Denn (2009); Bertola *et al.* (2003)]. Despite these hardships, the apparent yield stress is an engineering reality and an important feature from a manufacturing or utilization point

a)Author to whom correspondence should be addressed; electronic mail: norbert.willenbacher@kit.edu

of view. For example, the processing of ceramic materials, sagging of coatings or detergent foams, emptying and filling of containers for cosmetic or pharmaceutical emulsions, even texture and taste of food products are controlled by the apparent yield stress of these fluids. Numerous studies have addressed the yield stress phenomenon and its appropriate quantification [Bertola *et al.* (2003); Coussot (2005); Piau and Piau (2007); Prud'homme and Khan (1996)]. For instance, it has been shown that for densely packed emulsions, τ_y is closely related to droplet deformability and accordingly is determined by the packing density and the Laplace pressure of the droplets [Princen and Kiss (1986)]. Despite the strong elongational components that exist in complex flow fields of most technical processes, the vast majority of experimental studies deals with simple shear flow. The orifice extrusion method has been used to determine the elongational yield stress $\tau_{y,e}$, e.g., of soap pastes [Castro *et al.* (2010)], but this technique is not sensitive enough for the soft matter systems addressed here. Capillary break-up elongational rheometry (CaBER) has also been employed to determine the yield stress of soft matter. In these experiments, the thinning and break-up of a stretched filament due to the action of the surface tension is monitored. Theoretical predictions for the time evolution of the filament diameter $D(t)$ have been derived for Bingham [McKinley (2005)] as well as for Herschel-Bulkley fluids [Tiwari *et al.* (2009)]. They assume first homogeneous deformation of a cylindrical filament and second a vanishing stress in the direction of the filament axis ($\tau_{xx} = 0$). In a recent study on carbon nanotube suspensions, yield stress values obtained from the evaluation of CaBER data based on the above mentioned analysis did deviate significantly from the values obtained by classical shear experiments [Tiwari *et al.* (2009)]. However, it has to be kept in mind that yield stress fluids exhibit a strong necking, i.e., the cylindrical filament assumption is not fulfilled. Furthermore, it is not clear whether $\tau_{xx} = 0$ is valid in that case. An accurate description of $D(t)$ curves from CaBER experiments for yield stress fluids requires the numerical solution of the full axial symmetric two-dimensional flow problem with appropriate boundary conditions.

Here, we use a method to determine the elongational yield stress that is especially suitable for soft complex fluids with apparent yield stresses in the range from 0.1 to 100 Pa. The method is based on the observation that yield stress fluids can form stable cylindrical bridges with lengths larger than the cylinder circumference called filaments. The onset of filament deformation and flow is determined by the yield stress [Mahajan *et al.* (1999); Lowry and Steen (1995)]. This approach does not require the assumption of any particular constitutive equation.

A cylindrical fluid element is exposed to a step strain elongational deformation. As long as the stress within the fluid is below the yield value, the filament shape does not change and the Laplace pressure within the liquid thread, calculated from its radius and axial curvature at the midpoint, is identified as the elongational yield stress $\tau_{y,e}$. In contrast to our previous study on a series of w/o-emulsions [Niedzwiedz *et al.* (2010)], we find that filaments always break, but the break-up time strongly depends on the step strain. We define a Deborah number as the ratio of the characteristic intrinsic relaxation time of the fluid and the filament lifetime. The ratio of elongational to shear yield stress is then discussed in terms of this dimensionless number. The proposed experimental approach can be applied to a wide class of materials including dispersions, emulsions, and foams as well as numerous technically important complex formulations as construction materials, coatings, adhesives, personal care products, pharmaceuticals, and food products. Here we present data for different polymeric gels, flocculated suspensions, as well as highly concentrated, densely packed emulsions including thoroughly characterized model systems and various commercial products. Systematic investigations of $\tau_{y,e}$ provide new fundamental insight into the yielding and flow of such materials.

II. THEORETICAL BACKGROUND

The Herschel-Bulkley model is widely used to describe the flow behavior of yield stress fluids on a continuum mechanical level [Herschel and Bulkley (1926)]

$$\tau_{xy} = \tau_{y,s} + k\dot{\gamma}^n, \tag{1}$$

where τ_{xy} is the shear stress, $\tau_{y,s}$ is the shear yield stress, k is the consistency index, $\dot{\gamma}$ is the shear rate, and n is the shear thinning exponent. The following relationship between the extra-stress tensor $\mathbf{T}$ and the strain-rate tensor $\mathbf{D}$ has been used to analyze the behavior of yield stress fluids in complex flow fields [Castro *et al.* (2010); Tiwari *et al.* (2009); Basterfield *et al.* (2005); Alexandrou *et al.* (2003); Adams *et al.* (1997); Coussot and Gaulard (2005)]:

$$\mathbf{T} = 2\left[\frac{\tau_{y,s}}{\sqrt{|II_D|}} + k\left(\sqrt{|II_D|}\right)^{n-1}\right]\mathbf{D}, \tag{2}$$

where II_D is the second invariant of the strain tensor. In simple shear flow, $\mathrm{II}_D = 1/2[(tr2\mathbf{D})^2 - tr(2\mathbf{D})^2] = -\dot{\gamma}$ and Eq. (2) reduces to Eq. (1). In uniaxial elongation $\mathrm{II}_D = -3\dot{\varepsilon}^2$, with $\dot{\varepsilon}$ the elongation rate, and for $\dot{\varepsilon} > 0$, the first normal stress difference reduces to

$$\tau_{xx} - \tau_{yy} = \sqrt{3}(\tau_{y,s} + k(\sqrt{3}\dot{\varepsilon})^n), \tag{3}$$

which corresponds to a constant relationship between elongational and shear yield stress

$$\tau_{y,e} = \sqrt{3}\tau_{y,s}. \tag{4}$$

This relationship is in agreement with the von Mises plasticity criterion [Coussot (2005)], which predicts the yielding of materials under arbitrary loading conditions and suggests that materials do not flow as long as the second invariant of the extra-stress tensor does not exceed a critical value

$$\sqrt{|\mathrm{II}_T|} < \tau_c. \tag{5}$$

This criterion and hence also Eq. (4) has been experimentally confirmed for plastic solids or pastes with very high yield stresses [Castro *et al.* (2010); Basterfield *et al.* (2005); Adams *et al.* (1997)]. The behavior of yield stress fluids in complex flow fields including strong extensional components has been treated computationally with respect to a variety of different technical processes, e.g., gravity driven dripping from a nozzle [Coussot and Gaulard (2005)]. Plastic flow of semisolid materials like aluminum slurries has been analyzed numerically for complex flow kinematics using the Bingham as well as the Herschel-Bulkley model with respect to the processing of ceramic materials [Alexandrou *et al.* (2003); Alexandrou (2008); Alexandrou and Georgiou (2007)]. In all these simulations, the contribution of the third invariant of the strain-rate tensor has been tacitly neglected and the Herschel-Bulkley model has been used as given in Eq. (2).

Recently, a statistical mechanical model based on mode coupling theory has been proposed to predict the nonlinear flow behavior of dense colloidal suspensions close to the colloidal glass transition [Brader *et al.* (2008, 2009)]. This model also confirms the von Mises phenomenological criterion and Eq. (4) is recovered for suspensions in the glassy

state. But so far, systematic investigations on the relationship between shear and elongational yielding of soft matter like dispersions, emulsions, and foams are still lacking. The validity of such a general relationship for the ratio of the elongational and shear yield stress like Eq. (4) is not so obvious as the physical origin of the yielding phenomenon in this broad variety of fluids may be very different.

From a continuum mechanical point of view, the generalization of Eq. (1) to Eq. (2) is not straight forward, but tacitly assumes that the extra-stress tensor is independent of the third invariant of the strain-rate tensor $\mathrm{III}_D = \det(2\mathbf{D})$. Recently, a generalized Herschel-Bulkley constitutive equation including III_D which fulfills the general requirements for a Reiner-Rivlin fluid [Graebel (2007)] has been proposed [Niedzwiedz *et al.* (2010)]

$$\mathbf{T} = 2\left[\frac{\tau_{y,s}}{\sqrt{|\mathrm{II}_D|}+m_1\sqrt[3]{\frac{\mathrm{III}_D}{2}}} + k\left(\sqrt{|\mathrm{II}_D|} + m_2\sqrt[3]{\frac{\mathrm{III}_D}{2}}\right)^{n-1}\right]\mathbf{D}. \tag{6}$$

This constitutive equation includes the material parameters m_1 and m_2, which are irrelevant in shear experiments, for which $\mathrm{III}_D = 0$, but result in a nontrivial relationship between the yield stress determined in shear and uniaxial extensional flow

$$\tau_{y,e} = \frac{3\tau_{y,s}}{\sqrt{3}+m_1}. \tag{7}$$

If the contribution of III_D is neglected (i.e., $m_1 = m_2 = 0$), Eqs. (6) and (7) reduce to Eqs. (2) and (4).

III. MATERIALS

A wide range of materials with different origin of the yield stress have been investigated. These include polymeric gels with physical and chemical crosslinks, highly concentrated emulsions, and aggregated suspensions with attractive particle interactions.

A. Polymers

Two synthetic polymeric thickeners Sterocoll D and Viscalex H30 both provided by BASF SE have been used. They are made from emulsion polymerization and are supplied as milky, aqueous dispersions with a solid content of about 25% and a *p*H of 2.2–2.6. Their main monomers are ethylacrylate and (meth)acrylic acid. Sterocoll D additionally includes a small fraction of diethylenically unsaturated monomer as chemical crosslinker and Viscalex HV30 includes hydrophobic side chains providing physical crosslinking in aqueous solution.

Neutralized aqueous solutions with different polymer concentrations between 1 and 5 wt. % have been prepared as described by Kheirandish *et al.* (2009). Two Viscalex HV30 solutions have been neutralized with sodium hydroxide (concentration of polymers: 0.97% and 1.84%), and one Viscalex HV30 solution has been neutralized with triethanolamine (polymer concentration: 3.18%), which results in distinctly different rheological behavior. Furthermore, a commercial hair gel Gard Style (Doetsch Grether AG, Switzerland) has been investigated. Since the yield stress of the original hair gel was too high to be used in CaBER experiments, the gel was diluted to 4 and 2.2 wt. % solids content with deionized (DI) water. The major polymeric ingredients are poly(vinylpyrrolidone) and polyquaternium-86.

B. Suspensions

Precipitated and hydrophobically modified calcium carbonate ($CaCO_3$) particles Socal (Solvay Advanced Functional Materials, France) as well as hydrophobically modified glass beads have been suspended in di-isononylphtalate (DINP) with $\eta = 72$ mPa s using a Heidolph RZR 2020 stirrer as described by Koos and Willenbacher (2011).

Hydrophobic precipitated silica particles Sipernat D17 (Evonik, Germany) have been dispersed in silicone oil AK1000 (Wacker, Germany) with $\eta = 1000$ mPas using an ultrasonic device (Branson Sonifier 250). Ultrasonification lasted for 1 h. The average particle diameter is 1.8 μm (Socal), 25 μm (glass beads), and 3 μm (Sipernat D17) and the particle volume fraction in the suspensions is $\phi = 0.33$ (Socal), 0.4 (glass beads), and 0.27 (Sipernat D17). In all cases, the particle loading is well below the maximum packing fraction, but due to attractive van der Waals interactions, particles form a sample spanning network, which results in an apparent yield stress.

C. Emulsions

Two commercial cosmetic emulsions Nivea Body Milk and Nivea Soft Crème both provided by Beiersdorf AG (Germany) have been investigated. The Body Milk is a highly concentrated w/o-emulsion, its internal phase volume fraction is $\phi = 0.75$, and the average droplet diameter is $D = 0.9$ μm [Niedzwiedz *et al.* (2009)]. The Soft Crème is an o/w-emulsion with $\phi = 0.35$, the droplet size distribution is narrow, and $D \approx 0.9$ μm. The main constituent of the internal phase is paraffin oil ($\eta = 230$ mPas). In this case, the rheological features are mainly controlled by a proprietary mixture of surfactants and other water soluble ingredients.

Another emulsion has been prepared using paraffin oil as continuous phase, Span 80 (Merck) as a surfactant, and a water/glycerol mixture (60:40 by weight, $\eta = 11$ mPas) as internal phase. First, the surfactant was added to the oil phase during continuous stirring for 5 min, then the water/glycerol mixture was slowly added while stirring for additional 15 min. The resulting emulsion had a broad droplet size distribution with an average diameter $D = 20$ μm; the continuous phase volume fraction was $\phi = 0.47$.

Furthermore, a series of Pickering emulsions with different internal phase volume fraction has been made using the above mentioned water/glycerol mixture as disperse and the paraffin oil as continuous phase. The surfactant Triton X-100 (Carl Roth) has been mixed with the water/glycerol mixture at a weight fraction of 0.02% using a propeller stirrer. The hydrophobic silica particles Sipernat D17 have been added to the continuous oil phase at a weight fraction of 5% as described above. This resulted in emulsions with broad particle size distribution with an average droplet diameter of about 10 μm. For different emulsions with internal phase volume fractions between 0.17 and 0.52 have been prepared. The silica particles not only cover the water/oil interface but also form a network structure spanning the continuous phase connecting the dispersed droplets, and this particular structure gives rise to an apparent yield stress.

IV. METHODS

A. Shear measurements

Shear experiments were performed using a controlled stress rheometer (HAAKE Rheostress RS 150, Thermo HAAKE, Germany) equipped with a plate-plate geometry at ambient temperature. Rough plates were systematically used as slippage was noticed for some materials, and the gap width was always chosen to be 1 mm.

The characteristic shear relaxation time of the fluids was determined from oscillatory shear experiments as follows: First, a stress amplitude sweep was performed at a reference frequency of 0.1 Hz in order to determine the linear viscoelastic regime. The appropriate stress amplitude range was material dependant, but typically the stress was varied between 0.3 and 10 Pa or between 0.3 and 100 Pa. A frequency sweep was then run at a selected stress corresponding to the linear viscoelastic regime in order to determine the storage modulus G′ and the loss modulus G″. Depending on material, the frequency range was $10^{-3} < \omega < 10$ rad/s. Then the material relaxation time was identified as the inverse of the angular frequency ω at which G′ equals G″, i.e., $t_R = 1/\omega_{G'=G''}$. For some materials, like the aggregated suspensions or Pickering emulsions, this crossover was not directly accessible in the frequency range covered here. Then the crossover frequency was estimated from the decreasing G′ and increasing G″ at the lowest frequencies applied. For the Sterocoll D solutions and the Nivea Body Milk emulsion, strain-rate-frequency superposition (SRFS) was used to expand the frequency range down to 10^{-6} rad/s, thus enabling the determination of $\omega_{G'=G''}$ as described by Kowalczyk *et al.* (2010).

Stress ramps were used for a first estimate of the apparent yield stress. Depending on the material, the applied shear stress varied between 0.5 and 50 Pa or between 5 and 500 Pa within 300 s and the corresponding viscosity was recorded.

Then two different methods were used to determine the shear yield stress more precisely.

First, the shear yield stress was deduced from creep tests as described by Nguyen and Boger (1992). A constant shear stress was applied during 300 s and the resulting deformation was recorded. This protocol was repeated for several shear stresses below and above the estimated yield value. At low stresses, the compliance $J = \gamma/\tau_{xy}$ calculated from the applied shear stress and the deformation γ approached a constant value at long times. On the contrary, J remained time dependent even at long times and exhibited a linear time dependence when the yield point was exceeded.

Second, the shear yield stress was obtained from oscillatory shear measurements as described by Barnes (1999) and Nguyen and Boger (1992). For all investigated materials, a frequency range was found in which the materials behavior was predominantly elastic, i.e., G′ is independent of frequency and much larger than G″. A frequency corresponding to this elastic regime was selected and a stress amplitude sweep was performed at this frequency. The yield stress was then determined as the stress at which G′ equals G″ in the nonlinear response regime, where G′ decays and G″ goes through a maximum. The yield stress determined according to this protocol did not depend on frequency, as long as the frequency was selected in the elastic response regime, which typically ranged from 0.01 to 10 Hz.

This second approach is less time consuming and provides accurate and reproducible results.

Prior to the oscillatory or creep experiments, samples were exposed to a steady preshear for 2 min at $\dot{\gamma} = 100\,\mathrm{s}^{-1}$ and then left at rest for at least 10 min.

The thixotropic behavior of materials was tested using oscillatory shear rheometry. The storage modulus G′ was determined in the frequency range between 0.1 and 10 Hz; data were recorded directly after 2 min preshear at $\dot{\gamma} = 100\,\mathrm{s}^{-1}$ and then again after 10 min at rest. The corresponding moduli were compared.

B. Elongational measurements

To determine the elongational yield stress of soft matter, a small volume of material was placed between two parallel plates, which were subsequently stretched from their

initial separation height h_0 to a final height h_f within a stretching time t_s. For each selected stretch ratio $\varepsilon = h_f/h_0$, the filament shape was monitored during a preselected time. At first, the filament seems to be in a metastable state and its shape changes only very slowly. But, at a critical time depending on both the material and the applied stretch ratio, the filament suddenly shrinks and rapidly breaks. The Laplace pressure Δp within the liquid thread is related to the radius R and the axial curvature κ of the filament

$$\Delta p(x,t) = \Gamma_s \left(\frac{1}{R(x,t)} - \kappa(x,t) \right), \tag{8}$$

with

$$\kappa(x,t) = \left| \frac{\left(\partial^2 R(x,t)/\partial x^2 \right)}{\left[1 + (\partial R(x,t)/\partial x) \right]^{3/2}} \right|,$$

where Γ_s is the surface tension. Measurements were performed with a Capillary Breakup Elongational Rheometer (CaBER 1, Thermo HAAKE, Germany) as described by Niedzwiedz *et al*. (2010, 2009). Experiments were carried out at ambient temperature of about 20 °C.

A default plate diameter $D = 6$ mm and a default plate separation $h_0 = 1.5$ mm was selected. However, the ratio $r = h_0/D$ was varied by varying both h_0 from 1 to 2 mm and D from 4 to 8 mm without noticing any significant impact on the Laplace pressure subsequently determined in the stretched filament. For illustration, the evolution of the Laplace pressure within a filament of Sterocoll D 3% for $r = 0.25$ and $r = 0.33$ is shown in Fig. 7.

The upper plate was moved from its initial position h_0 to its final position h_f within a default stretching time $t_s = 0.48$ s. The final height h_f was varied for each material, which resulted in a filament lifetime variation. The Hencky strain rate $\dot{\varepsilon} = \ln(h_f/h_0) \times 1/t_s$ corresponding to this step stretch deformation varies weakly with the stretch ratio and is on the order of 1 s^{-1}. Three tests were performed for each material and each stretch ratio.

The subsequent filament thinning process was captured by a high-speed camera Fastcam-X 1024 PCI (Photron USA, Inc.) with a sampling speed of 125 frames per second. The resolution of each frame was 1024×1024 pixels. The camera was equipped with telecentric optics providing a spatial resolution of 16 μm [Niedzwiedz *et al*. (2009)]. To improve contrast, the fluid filament was illuminated from the back with a telecentric monochromatic blue light.

For each experiment, several sets of 160 frames were regularly recorded until the filament breakup. The time separating two sets of frames was adjusted to cover the whole filament lifetime. This procedure was chosen due to data storage restrictions of the camera. Image analysis provided the transient filament diameter over the full filament length. Both rims of the filament were detected based on the algorithm described by Niedzwiedz *et al*. (2009). Then, both the minimum diameter and the curvature at this filament height were deduced from experimental data using standard MATLAB fitting functions. From these data, the Laplace pressure was calculated according to Eq. (8). The uncertainty in the Laplace pressure determination during a single experiment shows up in the scatter of data shown, e.g., in Fig. 8. From the Δp versus time curves, we have determined the initial plateau value and the filament lifetime. The average initial plateau of Δp is used to calculate $\tau_{y,e}$. The experimental error for this quantity, given in Table I, corresponds to the standard deviation of the three tests that have been run for each material and stretch ratio. The filament lifetime enters into the calculation of the Deborah number [Eq. (9)] and the

TABLE I. Experimental results for all the materials investigated here, the apparent shear yield stress has been obtained either from oscillatory shear (o) or creep experiments (c) as indicated in column four. For the polymeric systems, the polymer concentration is given in weight percentage and for the Pickering emulsions, the internal phase volume is provided in column one. The relative error in shear relaxation time and yield stress determination is typically about 10%. The error for the elongational yield stress was determined from the error of both curvature and surface tension measurements. For each material, surface tension error was determined as the standard deviation of 3–5 repeated measurements on the same sample. Curvature error was deduced from the standard deviation of two CaBER experiments performed on the same material and at the same stretching ratio.

Materials	Γ_s (mN/m)	t_R (s)	$\tau_{y,s}$ (Pa)	Experimental protocol	$\tau_{y,e}$ (Pa)	$\tau_{y,e}$ error (Pa)	$\tau_{y,e}/\tau_{y,s}$ (—)	$\tau_{y,e}/\tau_{y,s}$ error
Socal in DINP	50.1	10 000	45	o/c	96	2.3	2.13	0.22
Glass beads in DINP	46.5	1 000	18	o/c	44	1.6	2.44	0.21
Sipernat in silicone oil	25.0	3 000	6	o/c	9	1.2	1.50	0.25
Nivea Body Milk	43.1	1 250[a]	8	o/c	18	2.2	2.25	0.36
Pickering emulsion $\phi = 0.19$	39.1	1 000	9	c	17	1.2	1.89	0.23
$\phi = 0.37$	35.8	850	8	c	18	1.7	2.33	0.33
$\phi = 0.52$	36.9	850	26	o/c	46	1.0	1.77	0.18
Nivea Soft Crème	121.0	6 700	91	c	115	42.0	1.26	0.49
W/o emulsion	17.0	1 000	5	c	8	0.9	1.78	0.27
Hair gel 2.2%	37.2	1 000	4	o/c	7	1.9	1.75	0.51
Hair gel 4%	97.0	1 500	21	o	38	8.0	1.81	0.42
Viscalex HV30 0.97%	66	900	22	o	46	4.4	2.09	0.29
Viscalex HV30 1.84%	81.5	1 000	43	o	80	3.4	1.86	0.20
Viscalex HV30 3.18%[b]	73.5	800	54	o	105	6.4	1. 94	0.23
Sterocoll D 2%	42.3	910[a]	3	o	5	1.4	1.76	0.51
Sterocoll D 3%	42.1	830[a]	4	o	7	1.9	1.89	0.55
Sterocoll D 5%	39.7	250[a]	7.5	o/c	15.5	1.2	2.06	0.26

[a]These relaxation time data have been taken from Kowalczyk *et al*. (2010).
[b]This solution has been neutralized with triethanolamine for all other polymeric systems NaOH was used.

experimental error is again calculated as the standard deviation of the results from repeated tests.

The surface tension of each material was measured with a tensiometer DCAT 11 EC (Dataphysics, Germany) using a Wilhelmy plate. The surface tension of each sample was measured three times. The average surface tension is given in Table I.

It has to be noticed that the assessment of the shape of the stretched filament requires a smooth filament surface as shown in Fig. 1(a). This requirement is typically not fulfilled for materials with a yield stress $\tau_{y,s} > 150\,\text{Pa}$, as demonstrated in Fig. 1(b) for the commercial cosmetic emulsion Nivea Creme (Beiersdorf AG, Germany). In this case, the curvature could not be inferred from the profile due to its irregularity. Furthermore, high yield stresses involved some slippage at the interface with the upper plate, as shown in Fig. 1(c). To limit this effect, rough sanded plates were used.

The typical time evolution of the filament is shown in Fig. 2 for the aqueous solution of Viscalex HV30 with polymer concentration 3.18%. The upper row shows the formation of the filament during the step strain deformation. The lower row shows the characteristic shape of the concave filament in the metastable state and after breakup. Similar filament shapes were observed for the other investigated materials and also for the highly concentrated emulsions investigated previously [Niedzwiedz *et al*. (2010)].

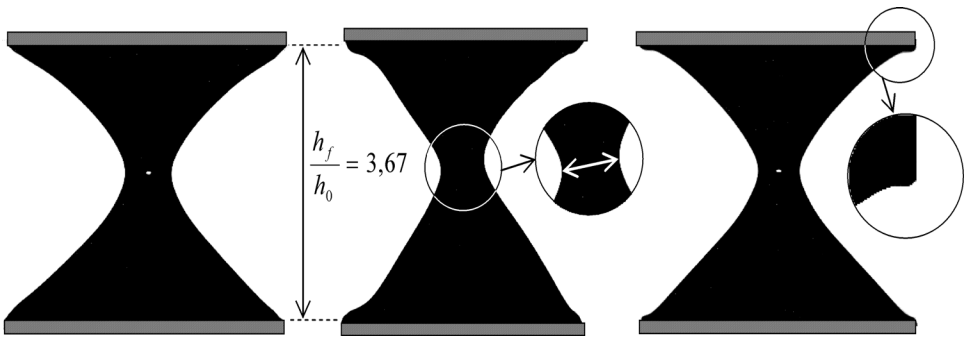

FIG. 1. Experimental filament profiles of the hair gel diluted to 4% polymer concentration obtained with rough (a) and smooth (c) plates. Filament profile of the cosmetic emulsion Nivea Crème with $\tau_{y,s} > 150\,\text{Pa}$ (b).

V. RESULTS AND DISCUSSION

A. Shear results

Characteristic shear relaxation times as well as apparent shear yield stresses were determined for all samples investigated here as described in Sec. IV. Although it is commonly accepted that suspensions or emulsions with attractive particle or droplet interactions, highly concentrated emulsions, and also polymeric microgel systems may exhibit apparent yield stresses [Larson (2009); Barnes (1999)], we show representative results from stress ramp, creep test, and oscillatory shear experiments for the materials investigated here. Figure 3 displays the viscosity obtained from stress ramp experiments as a function of shear stress for various materials. The materials selected are the suspension

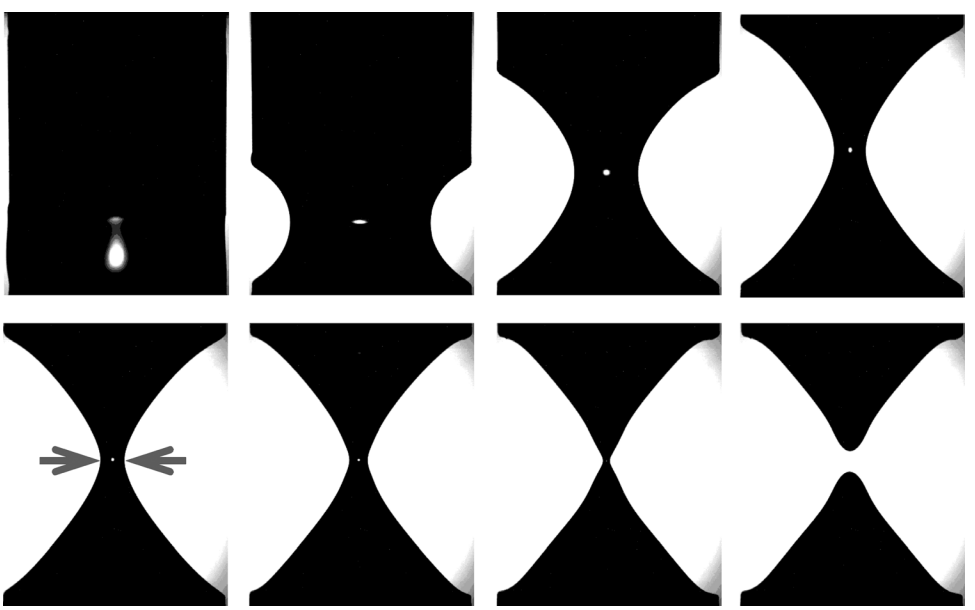

FIG. 2. Evolution of a filament profile for the Viscalex HV30 solution ($c_{\text{poly}} = 3.18\%$) stretched to a ratio $\varepsilon = 4.25$ within 0.48 s. (a) The upper pictures were recorded while the filament is being stretched. The lower pictures were recorded after the end of stretching. Cessation of motion of the upper plate is defined at $t = 0\,\text{s}$; the images were taken at $t = 60$, 491, 1043 s and $t > 1080\,\text{s}$. Filament breakup occurred at 1080 s. The gray arrows indicate where the minimum diameter is measured.

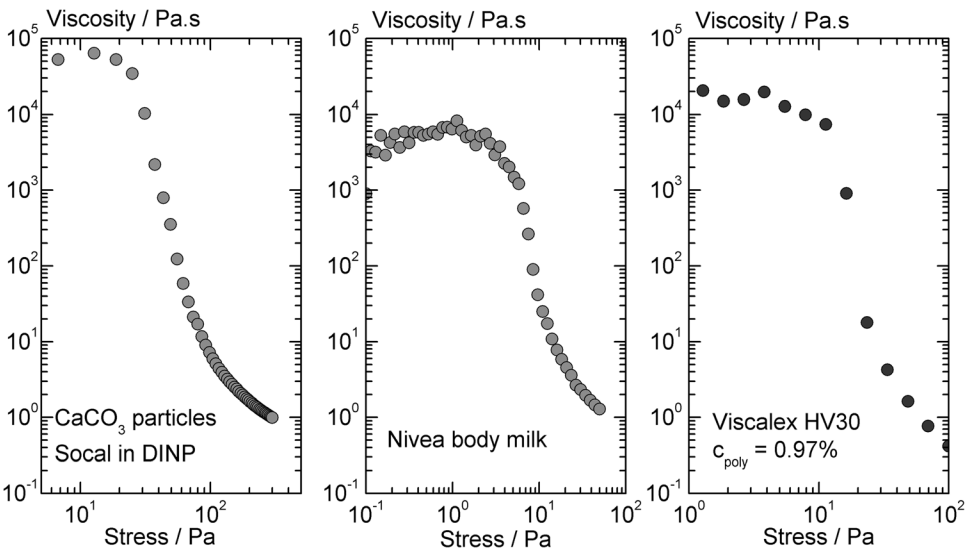

FIG. 3. Viscosity versus stress for a colloidal suspension of Socal in DINP (left), for the Nivea Body Milk emulsion (center) and for the Vicalex HV30 solution with $c_{\text{poly}} = 0.97\%$ (right). These curves come from stress ramp tests performed as described in Sec. IV.

of $CaCO_3$ particles in the organic solvent DINP, the highly concentrated emulsion Nivea Body Milk, and the microgel system Viscalex HV30 with 0.97% polymer concentration. All these data, set for very different materials, clearly show that there is a critical stress level or at least a narrow range of stresses at which the apparent viscosity changes drastically by several orders of magnitude. In that sense, these materials exhibit an apparent yield stress $\tau_{y,s}$. Nevertheless, irreversible flow processes take place even at stresses below $\tau_{y,s}$ and accordingly, the viscosity is high but not beyond the limit of measurability. It should be noted that the apparent zero shear viscosity at low stresses is not an equilibrium value, but depends on the time scale of the experiment as has already been pointed out previously for similar fluids [Moller *et al.* (2009)]. Nevertheless, the structural break down and the corresponding viscosity drop are always found at the same stress level irrespective of the experimental time scale.

For a more accurate determination of the yielding behavior, stress creep experiments have been performed at different stresses for each material. Typical results for the suspension of $CaCO_3$ particles in the organic solvent DINP, for the Pickering emulsion with the lowest particle loading $\phi = 0.168$, as well as for the hair gel with 2.2% polymer concentration, are shown in Fig. 4.

In all cases, we find a distinct change in deformation behavior with applied stress: Below the apparent yield point, the compliance approaches a constant value at long enough times, whereas it tends toward a linear increase with time at stresses above the yield stress. The apparent yield stress $\tau_{y,s}$ is thus defined as the lowest stress at which this linear increase in compliance is detected. For the polymeric systems, the constant compliance value is not always attained within the experimental window. Nevertheless, there is a critical stress value at which the compliance and its time dependence drastically change, justifying the term apparent yield stress. Alternatively, the yield stress has been determined from oscillatory shear experiments at varying stress amplitude. This approach is less time consuming than creep tests but also very accurate and reproducible. In this case, the stress at which G' equals G'' in the nonlinear response regime is defined as the

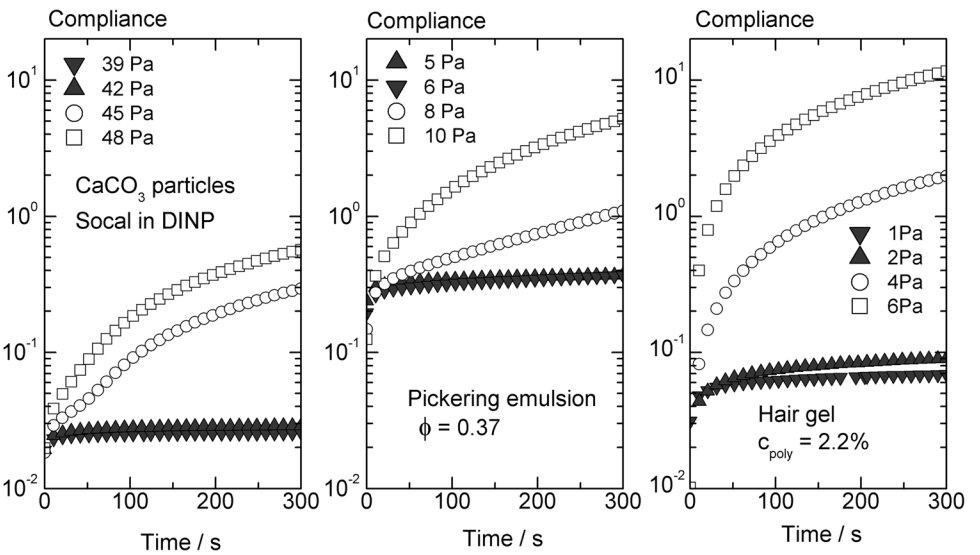

FIG. 4. Dependence of compliance on time for the Socal in DINP colloidal suspension (left), a Pickering emulsion with $\phi = 0.37$ (center), and a polymer solution of hair gel with $c_{\text{poly}} = 2.2\%$ (right). Data come from creep tests performed as described in Sec. IV. The apparent yield stress deduced from both oscillatory and creep tests are found equal to 45 Pa for Socal in DINP, 8 Pa for the Pickering emulsion ($\phi = 0.37$), and 4 Pa for the hair gel 2.2%.

yield stress. It should also be noticed that creep and oscillatory measurements provided a better repeatability of the resulting yield stress values than, e.g., fitting the Herschel-Bulkley model to experimental flow curves.

Representative results for the concentrated emulsion Nivea Body Milk are shown in Fig. 5. Obviously, the values $\tau_{y,s}$ are in excellent agreement. Similar results were obtained for all the materials investigated here. Finally, all yield stress values are summarized in Table I.

Furthermore, tests have been conducted to determine whether the materials investigated here are thixotropic or not. For that, the linear viscoelastic storage modulus G′ has

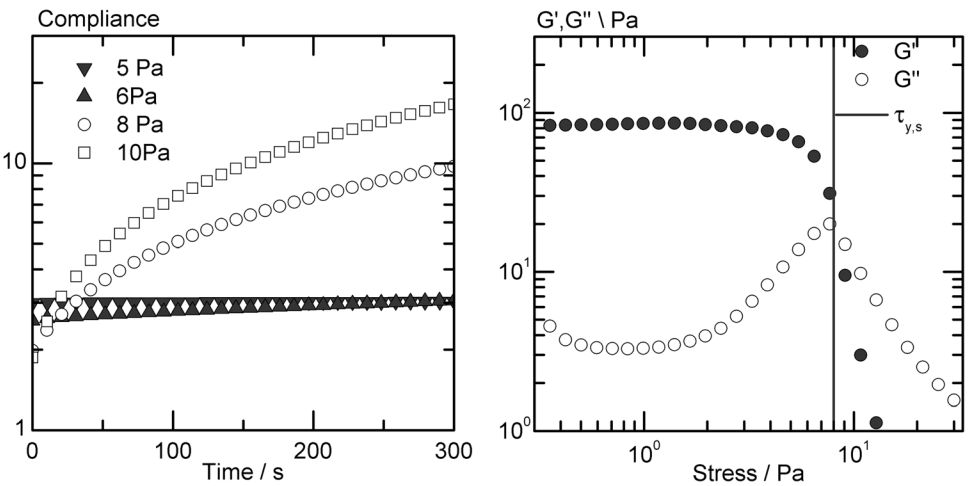

FIG. 5. Shear yield stress determination for Nivea Body Milk. Left: Compliance as a function of time from creep tests performed at different shear stresses. Right: Stress amplitude sweep at $f = 0.1$ Hz.

been measured for each material both directly after shearing the sample for 2 min at $\dot{\gamma} = 100\,\mathrm{s}^{-1}$ and after 10 min at rest. The relative change in G′ was typically around 10% and always below 40%. Thus, the materials were classified as nonthixoptropic.

Fluids with an apparent yield stress like the materials investigated here may nevertheless exhibit a finite characteristic relaxation time. This has been shown earlier for colloidal suspensions at the glass transition [Wyss *et al.* (2007); Siebenbürger *et al.* (2009)], densely packed emulsions, surfactant foams, and also polymeric microgel systems including the Sterocoll D solutions investigated here [Wyss *et al.* (2007), Kowalczyk *et al.* (2010)]. The characteristic relaxation time strongly depends on the material; it may be very long and thus difficult to access. The lower frequency limit in our oscillatory shear experiments was $\omega = 10^{-3}$ rad/s, corresponding to $t_R = 1000$ s. Typical G′ and G″ vs frequency data for a suspension, an emulsion, and a polymeric microgel system are shown in Fig. 6. For the Viscalex HV30 solutions, the Pickering emulsions and the suspension of glass beads in DINP t_R was taken as the inverse of the directly measured crossover frequency at which G′ = G″. For the Sterocoll D solutions and the Nivea Body Milk, it was shown earlier that the so-called strain rate frequency superposition principle originally introduced by Wyss *et al.* (2007) can be used to expand the accessible frequency range down to $\omega = 10^{-6}$ rad/s. For these systems, the existence of a crossover frequency and a terminal flow regime could be unequivocally demonstrated and the relaxation time data were taken from Kowalczyk *et al.* (2010). For the Nivea Soft Crème and the suspensions of Socal and Sipernat particles, no crossover was found within the experimental window and the SRFS principle could not be applied. In this case, the crossover was estimated from a linear extrapolation of the decaying G′ and the increasing G″ data in the low frequency range.

Finally, relaxation times between 10^2 and 10^4 s were found and apparent shear yield stresses ranged from about 1 to 100 Pa. These values are typical for soft glassy materials [Schall *et al.* (2007); Mason *et al.* (1995); Sollich *et al.* (1997); Cipelletti and Ramos (2005);

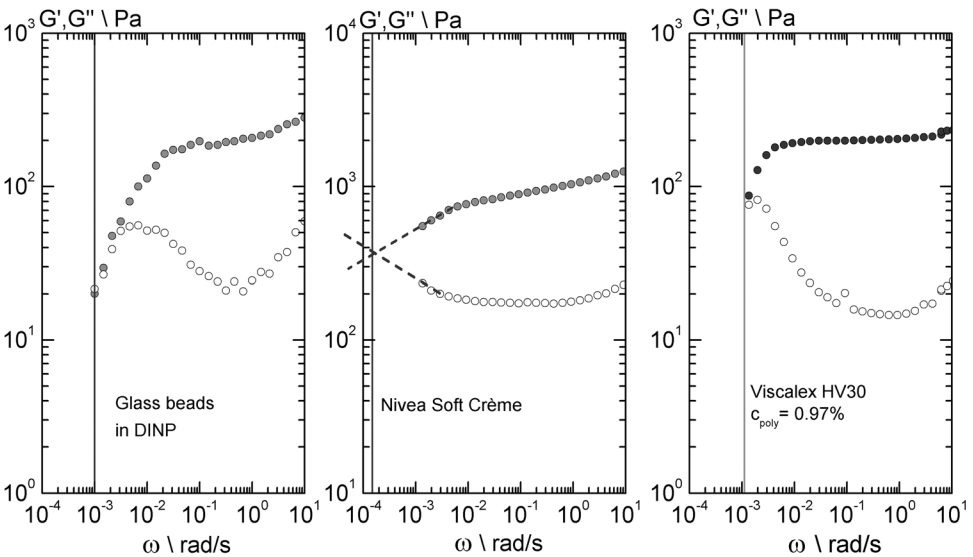

FIG. 6. Determination of the relaxation time for the suspension of glass beads in DINP (left), the Nivea Soft Crème emulsion (center), and a solution of Viscalex HV30 with $c_{\mathrm{poly}} = 0.97\%$ (right). Solid symbols represent G′, while open symbols represent G″. Vertical lines correspond to the crossover of G′ and G″. For the Nivea Soft Crème, the crossover has been extrapolated from the experimental data, as shown by the red dotted lines.

Banyopadhyay *et al*. (2010); Divoux *et al*. (2011)]. The counterintuitive decrease of relaxation time with increasing polymer concentration in the case of Sterocoll D can be attributed to the increase in ionic strength. It comes with the higher polymer concentration and has a strong influence on the subtle balance between intra- and intermolecular electrostatic repulsion and hydrophobic attraction, which determines the microstructure of these systems [Kheirandish *et al*. (2009)].

B. Filament stretching results

Several data sets for the transient Laplace pressure within a filament of the aqueous solution of the polymeric thickener Sterocoll D with a polymer concentration of 3 wt. % are superimposed in Fig. 7. Obviously, variation of plate diameter D, stretching time t_s, or the ratio $r = h_0/D$ does not have a major impact on the resulting Laplace pressure within the stretched filament. For this thickener solution, also the use of rough or smooth plates does not make a difference. However, this was not true for some other materials with higher yield stresses like the hair gel [see Fig. 1(c)], then rough plates were used. The time evolution of the Laplace pressure shown in Fig. 7 is typical for all fluids investigated here. First, the Laplace pressure remains constant for an extended period of time, but then Δp rapidly increases until the filament finally breaks. This essentially reflects the time evolution of the filament diameter, which decreases only weakly in the first period, but then rapidly decays until filament rupture.

The two parameters characterizing each test, namely the initial Laplace pressure plateau and the filament lifetime, depend on the stretching ratio ε, as shown on Fig. 8. The higher the stretching ratio ε, the higher the initial Laplace pressure level, and the lower the filament lifetime t_f. It is very important to notice that, no matter how small ε was

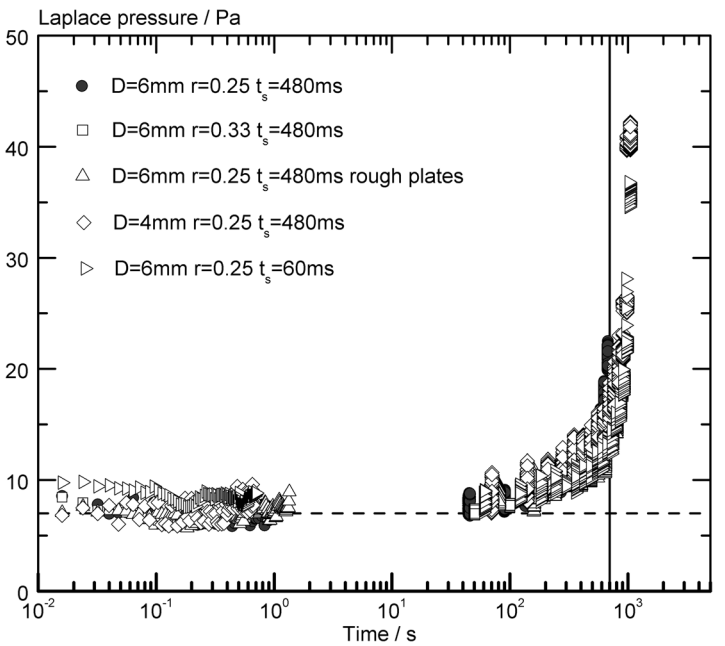

FIG. 7. Influence of various experimental parameters (plate diameter and roughness, stretching time) on the evolution of the Laplace pressure measured for a sample of Sterocoll D (3% polymer concentration) stretched between to opposite plates in a CaBER device. Red dots correspond to the reference experimental protocol. The vertical dashed line corresponds to a Deborah number of 1. The horizontal line indicates a stress of 7 Pa.

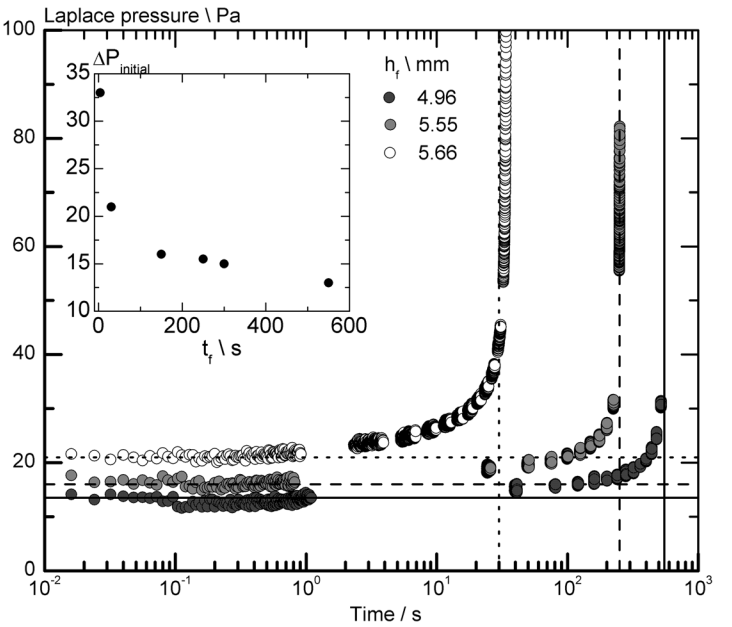

FIG. 8. Laplace pressure as a function of time for the sample Sterocoll D with $c_{poly} = 5\%$ at different stretch ratios. The vertical solid, dashed, and dotted lines indicate the filament lifetimes of 550, 250, and 30 s. The horizontal solid, dashed, and dotted lines indicate corresponding initial Laplace pressure values of 14, 16, and 21 Pa. The insert displays the evolution of Laplace pressure of all the available data for various filament lifetimes.

chosen, stretching always resulted in filament breakup and this was observed for all the fluids investigated here. The lowest stretch ratios at which the filament shape was continuously recorded was $\varepsilon = 2$. For some materials (Nivea Body Milk; Nivea Soft Crème; Viscalex HV30, $c_{poly} = 3.18\%$), filaments were kept overnight at even lower stretch ratios, but due to data storage restrictions of the camera, the filament shape was not recorded. Nevertheless, visual inspection after about 20 h confirmed that the filaments were broken. This means that the elongational yield stress cannot simply be deduced from the Laplace pressure within the filament at a critical stretching ratio at which the filament just does not yet break, as suggested in a previous paper [Niedzwiedz *et al.* (2010)]. Indeed, such a critical stretching ratio does not exist and may be falsely determined because of a too short time scale of observation.

Instead, an appropriate experimental time scale has to be considered. From an engineering point of view, this time scale may be set by a certain processing time of interest, e.g., the drying or curing time of a coating or the dispensing time for a cosmetic emulsion using a certain device.

From a material science point of view, being interested in a quantity which characterizes the elongational yielding of a given fluid, an intrinsic time scale distinctive for this particular fluid should be considered. Here, we select the longest shear relaxation time t_R as a genuine time scale and define a Deborah number

$$De = t_R / t_f. \tag{9}$$

Then, we perform several tests varying the stretching ratio to get the critical stretching ratio ε_c corresponding to a Deborah number $De \approx 1$. Finally, we define the initial plateau value of the Laplace pressure within the filament at ε_c as the apparent elongational yield stress $\tau_{y,e}$ of that material.

Setting the Laplace pressure within the filament equal to $\tau_{y,e}$ is justified assuming that the filament has a cylindrical shape and that $\tau_{xx} = 0$. The first assumption is well satisfied at the filament midpoint in the initial period after the step strain, which is relevant here. But it should be noted that this is no longer true when strong necking occurs and the filament rapidly shrinks prior to breakup. The validity of the second assumption is not so obvious, although it is frequently used in the analysis of CaBER experiments for many kinds of viscoelastic fluids. However, recent numerical simulations seem to confirm this assumption, particularly for yield stress fluids [Alexandrou *et al.* (private communication)]. Finally, it should be noticed that this determination of the elongational yield stress is fairly robust with respect to the choice of the timescale. An uncertainty in the determination of the shear relaxation time does not result in a strong variation of $\tau_{y,e}$. Exemplary this is demonstrated in the insert of Fig. 8 where the initial Laplace pressure is shown as a function of filament lifetime. Decreasing the stretch ratio resulted in a drop of t_f by almost 3 orders of magnitude from 4 to 1100 s, whereas Δp_{ini} varies by less than a factor of 3. Especially around $De = 1$, the initial Laplace pressure does not vary much. Similar results have been obtained for the other samples investigated here.

The curves shown in Fig. 8 exhibit the same shape and can be collapsed onto a single mastercurve by normalizing the Laplace pressure Δp by its initial value Δp_{ini} and the time t by the filament lifetime t_f. But even more than this, the shape of the curves measured for the different materials investigated here is also essentially the same as demonstrated in Fig. 9 for the polymeric systems, one emulsion and one suspension.

The ratio of the elongational to shear yield stress $\tau_{y,e}/\tau_{y,s}$ is plotted versus shear yield stress $\tau_{y,s}$ in Fig. 10. The corresponding data are summarized in Table I. This representation includes results for various physically very different fluids like polymeric gels, densely packed emulsions, or suspensions as well as suspensions with attractive

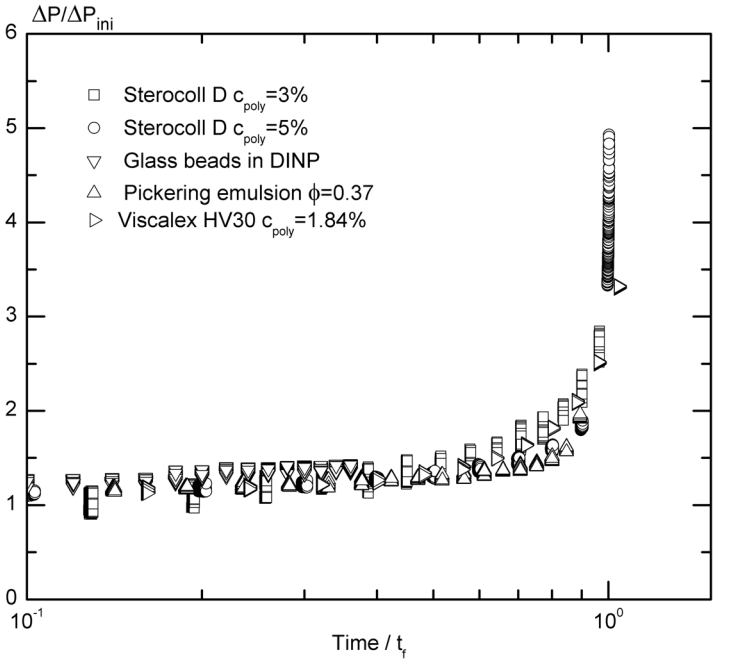

FIG. 9. Normalized Laplace pressure $\Delta P/\Delta P_{\text{ini}}$ as a function of time normalized by the filament lifetime t_f for two polymeric systems (Sterocoll D $c_{\text{poly}} = 3\%$ and 5%, Viscalex $c_{\text{poly}} = 1.84\%$), a Pickering emulsion ($\phi = 0.37$), and a colloidal suspension (glass beads in DINP).

interactions and roughly covers a shear yield stress range from 1 to 100 Pa. The elongational yield stress $\tau_{y,e}$ is determined from the Laplace pressure inside the stretched fluid at a Deborah number $De \approx 1$ as described above. Obviously, under these circumstances, the von Mises plasticity criterion is fulfilled and Eq. (4) holds within experimental uncertainty for the broad variety of fluids investigated here. Accordingly, Eq. (2) seems to be a useful three-dimensional constitutive relation, which can be used to model the yielding and flow of soft matter in complex flow kinematics.

So far, there has been little experimental evidence that the von Mises plasticity criterion is fulfilled for soft matter in complex flow kinematics. But recently, Ovarlez *et al.* (2010) reported experiments superimposing squeeze and rotational shear flow on similar soft matter (polymeric gel, emulsions). Their data show that unjamming the material in one direction leads to structural breakup in the perpendicular direction too. As a consequence, the onset of flow occurs when the root mean square of both shear stresses exceeds a critical value in agreement with Eq. (5). At a first glance, it seems to be surprising that the von Mises plasticity criterion, which was originally proposed for crystalline solids, is universally valid for so many different kinds of soft matter. But at least for dense colloidal suspensions, this criterion could be closely recovered from first principles. Based on mode coupling theory, Brader *et al.* (2008, 2009) have developed a constitutive equation for such systems, valid for arbitrary time-dependent but homogeneous flow kinematics and for uniaxial as well as planar extensional flow. $\tau_{y,e}/\tau_{y,s} \approx \sqrt{3}$ was found close to the colloidal glass transition.

From a process engineering point of view, the characterization of the elongational yield stress with respect to the materials relaxation time may not be most appropriate. Instead, it might be useful to consider a characteristic processing time or a deformation typical for a certain processing step or application technique. Therefore, we performed elongational deformation experiments at different stretching ratios ε, resulting in different

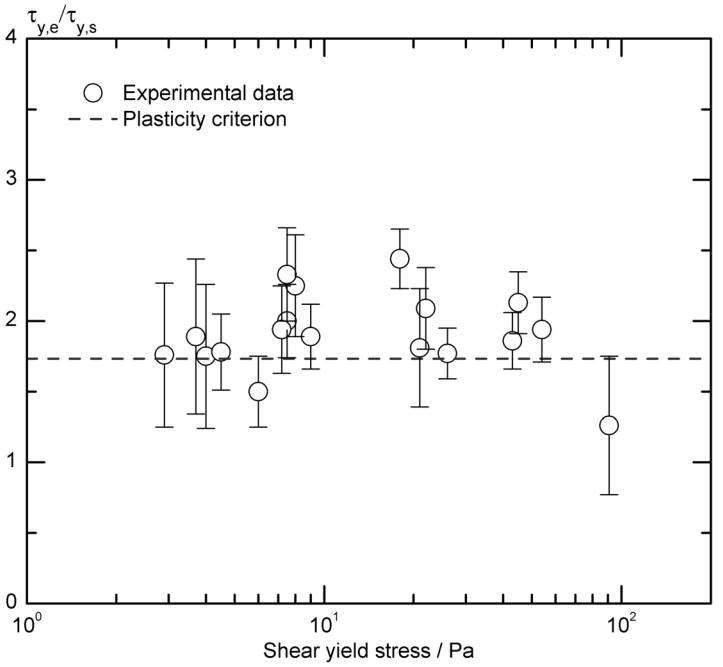

FIG. 10. Ratio of elongational to shear yield stress as a function of shear yield stress for the materials listed in Table I. The horizontal dashed line represents the von Mises plasticity criterion $\tau_{y,e}/\tau_{y,s} = \sqrt{3}$.

filament lifetimes. Accordingly, the initial plateau value of the Laplace pressure varies, i.e., it increases with increasing ε as shown in Fig. 8. The polymeric thickeners Sterocoll D and Viscalex HV30 and the highly concentrated emulsion Nivea Body Milk were selected for this investigation. Both polymer solutions were investigated at two different concentrations. The corresponding data for the ratio of the Laplace pressure to shear yield stress are displayed as a function of Deborah number in Fig. 11. Obviously, this ratio increases monotonically with increasing De. But it should be noted that for $De < 1$, this increase is weak and the normalized pressure varies only by about 1 order of magnitude while the Deborah numbers cover a range of three decades. Furthermore, the $\sqrt{3}$ ratio expected from the von Mises plasticity criterion [Eq. (5)] and from the simplified Herschel-Bulkley model neglecting contributions from the third invariant of the strain-rate tensor [Eq. (2)] is only found for $De \approx 1$. Nevertheless, the data obtained for the five different fluids investigated here fall onto a single mastercurve. This probably reflects a universal relationship between the stresses within a fluid and the Deborah number. Irrespective of that, at least for the materials investigated here, the generalized Herschel-Bulkley model proposed in Eq. (6) should be used for numerical simulations of processes including complex flow kinematics.

The parameter m_1 can then be determined from the experiments outlined above using Eq. (7). Here, m_1 is a monotonically decreasing function of De only, with $m_1\,(De = 1) = 0$ and $\lim_{De\to\infty} m_1 = -\sqrt{3}$. The parameter m_2 may be determined from regular CaBER experiments in combination with a numerical simulation of the filament thinning process based on Eq. (6), but this is beyond the scope of this paper.

Large Deborah numbers correspond to high stretching ratios for which we assume that the rest structure of the fluid is destroyed and the material cannot recover this structure

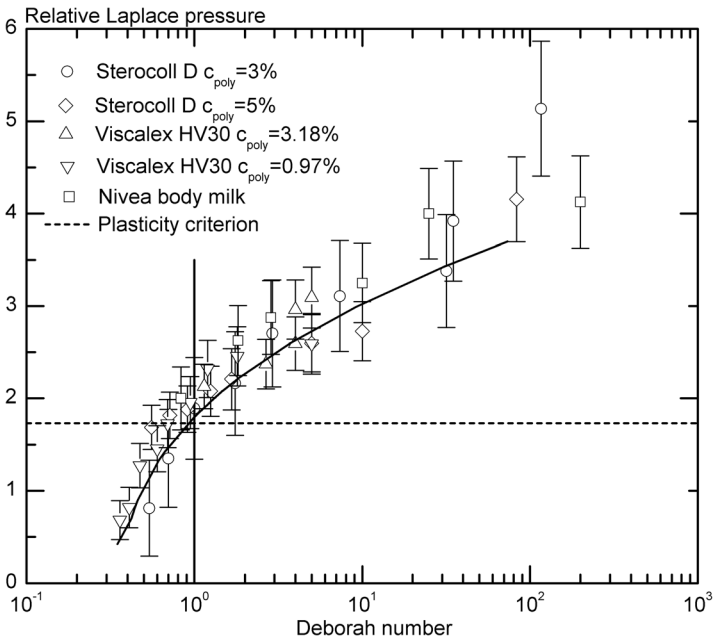

FIG. 11. Laplace pressure normalized to the corresponding shear yield stress vs Deborah number for different nonthixotropic yield stress fluids. Shear yield stress data were taken from Table I and it should be noted that in contrast to the apparent elongational yield stress the quantity $\tau_{y,s}$ does not depend on the selected experimental time scale relevant here. The solid line is to guide the eye, the horizontal line represents the von Mises plasticity criterion, and the vertical line marks $De = 1$.

within the experimental time scale. Thus the stress is predominately viscous and the stress ratio is about 3, close to what is expected for viscous Newtonian fluids. In a previous paper [Niedzwiedz *et al.* (2010)], we have reported $\tau_{y,e}/\tau_{y,s}$ values close to three for a series w/o emulsions. These data were obtained using essentially the same experimental approach as used here, but the Deborah number was larger than 10 in these experiments and thus these results agree well with those reported here. On the other hand, small Deborah numbers correspond to small deformations and the material responds elastically, then $\tau_{y,e}/\tau_{y,s} = \sqrt{3}$ at $De \approx 1$. For very low $De < 1$, i.e., weak deformations, oriented structural rearrangements during the time of experiment may be responsible for the low $\tau_{y,e}/\tau_{y,s}$ values.

VI. CONCLUSION

Here, we present a new approach to determine the apparent elongational yield stress of soft matter including polymer gels, highly concentrated emulsions, and aggregated suspensions. The apparent shear yield stress varies between 1 and 100 Pa and the longest shear time between 10^2 and 10^4 s for the broad variety of fluids investigated here. To determine the elongational yield stress, a cylindrical fluid element is rapidly stretched to a certain stretching ratio ε between two metal plates. In an initial period after the step strain, the Laplace pressure within the filament is essentially constant, but finally it increases rapidly and the filament breaks, for all the fluids investigated here. In all cases, filament lifetime strongly increases with decreasing stretching ratio. We define a Deborah number $De = t_R/t_f$. We finally identify the initial value of the Laplace pressure obtained at a critical value ε_c corresponding to $De = 1$ as the apparent elongational yield stress characterizing the uniaxial elongational yielding of a given material.

For all the investigated fluids, the ratio of this elongational yield stress to the shear yield stress is $\tau_{y,e}/\tau_{y,s} = \sqrt{3}$, in agreement with the von Mises plasticity criterion and irrespective of the physical nature of structural breakdown. Accordingly, the three-dimensional Herschel-Bulkley model, ignoring the contribution from the third invariant of the strain-rate tensor III_D [Eq. (2)] can be used to calculate the behavior of soft matter in complex flow kinematics.

From a process engineering or application point of view, this elongational yield stress referring to a material specific relaxation time may be inopportune. Instead, a characteristic processing time or deformation may be considered. Accordingly, elongational deformation experiments have been performed at different ε and hence t_f. The Deborah number was thus varied from $0.1 < De < 100$ and a universal relationship between the normalized initial plateau value of the Laplace pressure and De was observed for all investigated fluids. The Laplace pressure normalized to the shear yield stress was found to increase monotonically with increasing De. This ratio varied between 0.5 and 5 in the investigated De range and equals $\sqrt{3}$ only for $De \approx 1$. For large De, the stress ratio is close to 3. This latter finding can be rationalized assuming that the materials rest structure is destroyed at these large deformations. Then the stress within the fluid is predominantly viscous and the ratio of elongational to shear stress is about 3 as expected for Newtonian fluids.

ACKNOWLEDGMENTS

The authors would like to thank B. Hochstein for fruitful discussions and technical advices, A. Kowalczyk for her help in characterization of microgel suspensions, S. Strubel for introducing L.M. to the experimental setup, and C. Gür for his assistance in the lab.

References

Adams, M. J., İ. Aydina, B. J. Briscoea, and S. K. Sinha, "A finite element analysis of the squeeze flow of an elasto-viscoplastic paste material," J. Non-Newtonian Fluid Mech. **71**, 41–57 (1997).

Alexandrou, A. N., "On the modeling of semisolid suspensions," Solid State Phenom. **141–143**, 17–23 (2008).

Alexandrou, A. N., and G. Georgiou, "On the early breakdown of semisolid suspensions," J. Non-Newtonian Fluid Mech. **142**, 199–206 (2007).

Alexandrou, A. N., P. Le Menn, G. Georgiou, and V. Entov, "Flow instabilities of Herschel–Bulkley fluids," J. Non-Newtonian Fluid Mech. **116**, 19–32 (2003).

Bandyopadhyay, R., P. H. Mohana, and Y. M. Joshi, "Stress relaxation in aging soft colloidal glasses," Soft Matter **6**, 1462–1466 (2010).

Barnes, H. A., "The yield stress—A review or $\pi\alpha\nu\tau\alpha\rho\epsilon\iota$ everything flows?," J. Non-Newtonian Fluid Mech. **81**, 133–178 (1999).

Basterfield, R. A., C. J. Lawrence, and M. J. Adams, "On the interpretation of orifice extrusion data for viscoplastic materials," Chem. Eng. Sci. **60**, 2599–2607 (2005).

Bertola, V., F. Bertrand, H. Tabuteau, D. Bonn, and P. Coussot, "Wall slip and yielding in pasty materials," J. Rheol. **47**, 1211–1226 (2003).

Bonn, D., and M. M. Denn, "Yield stress fluids slowly yield to analysis," Science **324**, 1401–1402 (2009).

Brader, J. M., M. E. Cates, and M. Fuchs, "First-principles constitutive equation for suspension rheology," Phys. Rev. Lett. **101**, 138301 (2008).

Brader, J. M., T. Voigtmann, M. Fuchs, R. G. Larson, and M. E. Cates, "Glass rheology: From mode-coupling theory to a dynamical yield criterion," Proc. Natl. Acad. Sci. U.S.A. **106**, 15186–15191 (2009).

Castro, M., D. W. Giles, C. W. Macosko, and T. Moadell, "Comparison of methods to measure the yield stress of soft solids," J. Rheol. **54**, 81–94 (2010).

Cipelletti, L., and L. Ramos, "Slow dynamics in glassy soft matter," J. Phys.: Condens. Matter **17**, R253–R285 (2005).

Coussot, P., *Rheology of Pastes, Suspensions and Granular Materials: Applications in Industry and Environment* (John Wiley Sons, Inc., Hoboken, New Jersey, 2005).

Coussot, P., and F. Gaulard, "Gravity flow instability of viscoplastic materials: The ketchup drip," Phys. Rev. E **72**, 031409 (2005).

Divoux, T., C. Barentin, and S. Manneville, "From stress-induced fluidization processes to Herschel-Bulkley behaviour in simple yield stress fluids," Soft Matter **7**, 8409–8418 (2011).

Graebel, W. P., *Advanced Fluid Mechanics*, (Academic Press, Burlington, MA, 2007).

Hartnett, J. P., and R. Y. Z. Hu, "Technical note: The yield stress—An engineering reality," J. Rheol. **33**, 671–679 (1989).

Herschel, W. H., and R. Bulkley, "Konsistenzmessungen von Gummi-Benzollösungen," Kolloid Zeitschrift **39**, 291–300 (1926).

Kheirandish, S., N. Willenbacher, and I. Gubaydullin, "Shear and elongational flow behavior of acrylic thickener solutions. Part II: Effect of gel content," Rheol. Acta **48**, 397–407 (2009).

Koos, E., and N. Willenbacher, "Capillary forces in suspension rheology," Science **331**, 897–900 (2011).

Kowalczyk, A., B. Hochstein, P. Stähle, and N. Willenbacher, "Characterization of complex fluids at very low frequency: Experimental verification of the strain rate-frequency superposition (SRFS) method," Appl. Rheol. **20**, 52340 (2010).

Larson, R. G., (2009), *The Structure and Rheology of Complex Fluids* (Oxford University Press, New York, 1999).

Lowry, B. J., and P. H. Steen, "Capillary surfaces: Stability from families of equilibria with application to the liquid bridge," Proc. R. Soc. London, Ser. A **449**, 411–439 (1995).

Mahajan, M. P., M. Tsige, P. L. Taylor, and C. Rosenblatt, "Stability of liquid crystalline bridges," Phys. Fluids **11**, 491–493 (1999).

Mason, T. G., J. Bibette, and D. A. Weitz, "Elasticity of compressed emulsions," Phys. Rev. Lett. **75**, 2051 (1995).

McKinley, G. H., in *Annual Rheology Reviews*, edited by D. M. Binding and K. Walters (British Society of Rheology, Aberystwyth, UK, 2005), p. 1.

Moller, P. C. F., A. Fall, and D. Bonn, "Origin of apparent viscosity in yield stress fluids below yielding," EPL **87**, 38004 (2009).

Niedzwiedz, K., H. Buggisch, and N. Willenbacher, "Extensional rheology of concentrated emulsions as probed by capillary breakup elongational rheometry (CaBER)," Rheol. Acta **49**, 1103–1116 (2010).

Niedzwiedz, K., O. Arnolds, N. Willenbacher, and R. Brummer, "How to characterize yield stress fluids with capillary breakup extensional rheometry (CaBER)," Appl. Rheol. **19**, 41969 (2009).

Nguyen, Q. D. and D. V. Boger, "Measuring the flow properties of yield stress fluids," Ann. Rev. Fluid Mech. **24**, 47–88 (1992).

Ovarlez, G., Q. Barral, and P. Coussot, "Three-dimensional jamming and flows of soft glassy materials," Nature Mater. **9**, 115–119 (2010).

Piau, M., and J. M. Piau, "Wall vibrations and yield stress–shear thinning coupling (small vibrational inertia)," J. Non-Newtonian Fluid Mech. **144**, 59–72 (2007).

Princen, H. M., and A. D. Kiss, "Rheology of foams and highly concentrated emulsions: III. Static shear modulus," J. Colloid Interface Sci. **112**, 427–437 (1986).

Prud'homme, R. K., and S. A. Khan, *Foams: Theory, Measurements and Applications* (Marcel Dekker, Inc., New York, 1996).

Schall, P., D. A. Weitz, and F. Spaepen, "Structural rearrangements that govern flow in colloidal glasses," Science **318**, 1895–1899 (2007).

Siebenbürger, M., M. Fuchs, H. Winter, and M. Ballauff, "Viscoelasticity and shear flow of concentrated, noncrystallizing colloidal suspensions: Comparison with mode-coupling theory," J. Rheol. **53**, 707–726 (2009).

Sollich, P., F. Lequeux, P. Hébraud, and M. E. Cates, "Rheology of soft glassy materials," Phys. Rev. Lett. **78**, 2020 (1997).

Tiwari, M. K., A. V. Bazilevsky, A. L. Yarin, and C. M. Megaridis, "Elongational and shear rheology of carbon nanotube suspensions," Rheol. Acta **48**, 597–609 (2009).

Wyss, H. M., K. Miyazaki, J. Mattsson, Z. Hu, D. R. Reichman, and D. A. Weitz, "Strain-rate frequency superposition: A rheological probe of structural relaxation in soft materials," Phys. Rev. Lett. **98**, 238303 (2007).